Date of publication xxxx 00, 0000, date of current version xxxx 00, 0000.

Digital Object Identifier 10.1109/ACCESS.2017.DOI

Accuracy Assessment and Cross-Validation of LPWAN Propagation Models in Urban Scenarios

MARTIN STUSEK[1, 2], DMITRI MOLTCHANOV[2], (Member, IEEE), PAVEL MASEK[1], (Member, IEEE), KONSTANTIN MIKHAYLOV[1, 3], (Senior Member, IEEE), OTTO ZEMAN[4], MARTIN ROUBICEK[4], YEVGENI KOUCHERYAVY[2], (Senior Member, IEEE), and JIRI HOSEK[1] (Senior Member, IEEE)

[1]Department of Telecommunications, Brno University of Technology, Brno, Czech Republic
[2]Unit of Electrical Engineering, Tampere University, Tampere, Finland
[3]Centre for Wireless Communications, University of Oulu, Oulu, Finland
[4]Vodafone Czech Republic a.s., Prague, Czech Republic

Corresponding author: Pavel Masek (e-mail: masekpavel@vutbr.cz)

For the research, the infrastructure of the SIX Center was used. This article is based upon support of international mobility project MeMoV, No. CZ.02.2.69/0.0/0.0/16_027/00083710 funded by European Union, Ministry of Education, Youth and Sports, Czech Republic and Brno, University of Technology. The described research was financed by the Technology Agency of the Czech Republic project No. TN01000007. The work of K. Mikhaylov has been supported by Academy of Finland 6G Flagship (grant 318927). Dmitri Moltchanov's work was supported by the Business Finland Project 5G-FORCE.

ABSTRACT With the proliferation of machine-to-machine (M2M) communication in the course of the last decade, the importance of low-power wide-area network (LPWAN) technologies intensifies. However, the abundance of accurate propagation models proposed for these systems by standardization bodies, vendors, and research community hampers the deployment planning. In this paper, we question the selection of accurate propagation models for Narrowband IoT (NB-IoT), LoRaWAN, and Sigfox LPWAN technologies, based on extensive measurement campaign in two mid-size European cities. Our results demonstrate that none of the state-of-the-art models can accurately describe the propagation of LPWAN radio signals in an urban environment. For this reason, we propose enhancements to the selected models based on our experimental measurements. Performing the fine-tuning of the propagation models for one of the cities, we select Ericsson Urban (NB-IoT, LoRaWAN) and 3GPP (Sigfox) models as the ones providing the closest match. Finally, we proceed to perform cross-validation of the propagation models using the data set for another city. The tuned models demonstrate an excellent match with the real data in the cross-validation phase. They outperform their competitors by at least 20 – 80 % in terms of relative deviation from the measured signal levels presenting the accurate option for NB-IoT, LoRaWAN, and Sigfox deployments planning in mid-size cities.

INDEX TERMS Accuracy assessment, city coverage, cross-validation, deployment planning, LoRaWAN, low-power wide-area networks, Narrowband IoT, propagation models, Sigfox

I. INTRODUCTION

Massive machine-type communications (mMTC) are expected to become a vital service in future 5G and beyond systems. Having drastically different design goals compared to conventional human-to-human (H2H) communications, mMTC service requires the deployment of specific radio access technologies known as a low-power wide-area network (LPWAN).

The LPWAN technologies recently introduced by the 3rd generation partnership project (3GPP), i.e., Narrowband IoT (NB-IoT) and LTE Cat-M1, as well as those introduced by third-parties (non-3GPP) such as Sigfox and LoRaWAN, are expected to be the key IoT enablers. LoRaWAN and Sigfox use the license-exempt frequency spectrum and advanced wireless technology approaches such as ultra narrowband (UNB) modulation for Sigfox and spread spectrum in the case of LoRaWAN to enable excellent communication range and low power communication. Nevertheless, they can not compete with the 3GPP-defined ones (NB-IoT and LTE Cat-M1) operating in the licensed spectrum concerning a maximum number of messages transmitted per day in both uplink

(UL) and downlink (DL) directions, transmission power or security mechanisms. See Table 1 for a more comprehensive comparison of LPWAN technologies in question.

TABLE 1: Key parameters of LPWAN technologies [1]–[6].

	LoRaWAN	Sigfox	NB-IoT	LTE Cat-M1
Coverage (MCL)	157 dB	162 dB	164 dB	155 dB
Technology	Proprietary (PHY), Open (MAC)	Proprietary	Open LTE	Open LTE
Spectrum	Unlicensed	Unlicensed	Licensed	Licensed
Frequency	433, 868, 915 MHz	868, 915 MHz	700-2100 MHz	700-2600 MHz
Bandwidth	125, 250, 500 kHz	100, 600 Hz	200 kHz	1.4 MHz
Max. ERP	14 dBm[2]	14 dBm[2]	23 dBm	23 dBm
Downlink data rate	0.3-50 kbps	0.6 kbps	0.5-27.2 kbps[1]	< 300 kbps
Uplink data rate	0.3-50 kbps	0.1-0.6 kbps	0.3-62.5 kbps[1]	< 375 kbps
Max. message size UL	242 B	12 B	1600 B	1600 B
Max. message size DL	242 B	8 B	1600 B	1600 B
Battery life	10+ years	10+ years	10+ years	10+ years
Module cost	6 $	3 $	12 $	19 $
Security	AES-128	AES-128	LTE Security	LTE Security

[1] The value is release-dependent (Rel. 13).
[2] The value of max. ERP is relevant for the EU.

Deploying the LPWAN systems is a challenging task as they have to satisfy not only capacity requirements but also provide ubiquitous coverage for various sets of indoor and outdoor applications. Therefore, the propagation models are vital tools used to plan the network (i.e., the locations of both base stations and end devices) and to estimate/predict the quality of service and communication performance. However, there are many propagation models that differ in their structure and factors hampering clear conclusions about their choice for a particular technology. This is especially important for complex city-scale urban deployments of LPWAN systems [7]. Therefore, the intended models cover the whole spectrum of primary sources, i.e., standardization, vendors/operators, and academia. From each group, we selected the most commonly referenced models in the literature, which are supposed to provide an accurate prediction in the whole operating spectrum of the selected LPWAN technologies (mainly sub-GHz band) [8]–[10].

A. MAIN CONTRIBUTIONS

In this paper, aiming to improve the accuracy of propagation models, which can be employed, e.g., for LPWAN deployments planning in an urban city environment, we have evaluated and improved the accuracy of standardized propagation models. To this aim, we start by over-viewing the standardized propagation models suitable for LPWAN technologies. Then we carry out an extensive measurement campaigns in two midsize European cities in the Czech Republic, i.e., Brno and Ostrava for three dominant LPWAN technologies: (i) NB-IoT, (ii) Sigfox, and (iii) LoRaWAN. Utilizing the results of our measurements, we propose and apply the two-steps refinement procedure based on the fine-tuning of models' parameters and cross-validation of the proposed propagation models.

The key contributions are:

- We show that none of the standardized models provide accurate approximation for considered LPWAN technologies and needs to be fine-tuned to match the specifics of urban environment.
- We deliver a methodology for fine-tuning of the propagation models for the LPWAN technologies basing on the experimental results. The utilization of proposed methodology is demonstrated and cross-validated for the two cities in the Czech Republic – Brno and Ostrava.
- The proposed and reported propagation models tuned using the real-life measurements outperform their competitors by at least 20 – 80 % in terms of relative deviation from the measured data.
- Finally, we give free access to our anonymized measurement results together with the created Matlab functions including the fine-tuned propagation models[1].

The rest of the paper is organized as follows. We first provide an overview of considered LPWAN technologies in Section II. The considered propagation models standardized for wireless technologies are summarized in Section III. The measurements campaign and obtained data sets are described and analyzed in Section IV. Further, the proposed evaluation methodology with cross-validation, model's quality assessment metric as well as numerical results identifying the best candidate models are provided in Section V. Conclusions are drawn in the last section.

II. LPWAN TECHNOLOGIES

In this section, we provide a brief overview of three major LPWAN technologies considered in our study, namely, (i) Sigfox, (ii) LoRaWAN, and (iii) NB-IoT. The first two representatives embody license-exempt technologies operating in the industrial, scientific and medical (ISM) band. The latter, on the other hand, stands for licensed LPWAN standard operating in long-term evolution (LTE) frequency spectrum.

A. SIGFOX

This technology operates within 200 kHz bandwidth in the ISM spectrum with a center frequency of 868 or 915 MHz based on geographical region. Each differential binary-phase shift keying (D-BPSK) modulated UL message covers 100 (all regions except the United States (US) and Latin America) or 600 Hz of the total bandwidth. It enables Sigfox to provide extended coverage over 10 km with a maximum throughput of 100 or 600 bps based on the utilized message bandwidth.

The use of the ISM band within the European region imposes duty-cycle (DC) restrictions of 1 % reflected by 140 UL messages with a maximum size of 12 B. The DL transmission is even more restricted with only 4 messages per day carrying 8 B payload. However, the regions with 600 Hz UL messages utilize a frequency hopping technique. The device broadcasts the message 3 times using 3 different frequencies (frequency hopping) with an on-time maximum of 400 ms per channel. No new transmission can be initiated before 20 s. In Japan and South Korea, the listen before talk (LBT) mechanism is utilized. The device has to verify that

[1] See https://github.com/martin146/ieee-access-data

the whole 200 kHz bandwidth is free of signals stronger than -80 dBm [3], [4].

B. LORAWAN

It is the second representative of license-exempt LPWAN technologies operating in the ISM band. LoRaWAN supports a wide variety of frequency bands, including 433, 868, and 915 MHz with an additional 500 and 780 MHz bands [11]. The physical layer of the LoRaWAN standard is based on proprietary long-range (LoRa) modulation complemented by the open medium access control (MAC) layer. The spreading factor (SF) parameter can adjust the robustness and throughput of the modulation; in total, six values ranging from 7 to 12 can be used.

Within the European 868 MHz band, the communication can use one of up to sixteen available channels with a bandwidth of 125 or 250 kHz. As in the case of the Sigfox, utilization of an unlicensed band limits the duty-cycle to 1 % of the operational period with the maximum radiated power of 14 dBm. These restrictions also affect the maximum message size that ranges from 51 B (SF12) up to 242 B (SF7) [5], [6]. In the US 915 MHz band, LoRaWAN utilizes a frequency hopping technique supporting 72 UL channels with bandwidth up to 500 kHz. The utilization of the 915 ISM band imposes the restrictions of 400 ms time-on-air interval allowing for the maximum SF10. As in the case of Sigfox, Japan and South Korea require LBT functionality [11].

C. NB-IOT

At the time of writing this paper, NB-IoT represents the only LPWAN technology operating in a licensed band, publicly available in the Czech Republic. NB-IoT is derived from the conventional LTE standard with which it shares a significant part of the infrastructure and numerology. This technology supports 13 different frequency bands (additional 4 and 7 bands in Rel. 14 and 15, respectively) ranging from 700 up to 2100 MHz. In contrast with LTE, it supports only half-duplex transmission with frequency division duplex (FDD). Thus, UL and DL communication is realized on a different frequency.

To achieve prolonged battery life, NB-IoT reduces the complexity of the communication modules in combination with power-saving mode (PSM) and extended discontinuous reception (eDRX). Utilization of licensed band allows for 23 dBm transmission power with message size up to 1600 B limited by the size of the protocol data unit (PDU). For UL transmission, NB-IoT utilizes 180 kHz bandwidth with 15 or 3.75 kHz sub-carriers spacing using single-carrier frequency-division multiple access (SC-FDMA). The whole bandwidth of NB-IoT fits in one physical resource block (PRB) of LTE. It allows NB-IoT to be deployed in three different ways: (i) inband occupying one PRB, (ii) in guardband of LTE band, or (iii) independently in a standalone mode. The UL message can be $\pi/2$-BPSK or $\pi/4$-QPSK modulated, enabling theoretical throughput up to 62.5 kbps (considering multi-tone transmission). The extended coverage of +20 dB (in comparison with LTE) is achieved mainly via the repetitions. In case of uplink communication, the message can be retransmitted up to 128 times [1], [2].

III. LPWAN PROPAGATION MODELS

The ability to accurately predict the radio signal behavior in given environment is a vital part of a network planning. The most common way to do so is to utilize propagation models. The propagation models for wireless technologies can be divided into three main categories: (i) empirical, (ii) deterministic, and (iii) stochastic, based on the derivation of the resulting path loss [12]. In this work, the main focus is on empirical models since they often feature a good balance between the accuracy and the computational performance.

A. MODELS REQUIREMENTS

To date, there is a plethora of propagation models proposed for wireless technologies originating from three primary sources: (i) standardization, (ii) vendors/operators, and (iii) academia. In our work, we focus on the propagation models covering the whole operational spectrum of the selected LPWAN standards, i.e., (i) Sigfox, (ii) LoRaWAN, and (iii) NB-IoT. Particularly, it covers a frequency range from 433 to 2100 MHz. LoRaWAN defines the lower bound of the frequency range, whereas NB-IoT delineates the upper limit. Even though NB-IoT can operate with a frequency slightly over 2 GHz, the sub-GHz frequencies are preferred due to better signal propagation which is the key requirement for the majority of LPWAN technologies [7].

Similarly to operational frequency, the channel bandwidth has a particular impact on signal propagation. Nevertheless, all the selected LPWAN technologies operate with decently narrowband signals ($<$ 200 kHz in most cases) compared to the carrier frequencies that often leads to frequency-flat fading [13]. According to that, we can consider only the carrier frequency and omit the channel bandwidth parameter.

Further, we also have to consider the physical layout of the LPWAN deployment. All the considered technologies rely upon a star topology (specifically, star-of-stars in case of the Sigfox and LoRaWAN) with the end devices (EDs) directly communicating to the base stations (BSs). The EDs are very often positioned slightly above ground level, albeit deployments below ground (e.g., in cellars) or above it (high-rise building) are also possible. Unlike the EDs, the antennas of the BSs in commercial deployments are often located high above the ground. The selected propagation models, therefore, need to address all the above-mentioned requirements to provide accurate results.

B. SELECTED MODELS

As already mentioned, for our analysis, we consider five extensively used propagation models with their basic parameters summarized in Table 2. The standardization group is represented by the 3GPP and COST 231 Wallfish-Ikegami (WI) models [14], [15]. The Ericsson propagation model [16] is an example of a vendor's group. Finally, the Okumura-Hata

and Stanford University Interim (SUI) propagation models are two widely known academic efforts in this area [10], [12].

TABLE 2: Basic parameters of selected propagation models.

Model	Frequency	BS Ht.	ED Ht.	BS-ED Dist.
3GPP	< 2600 MHz	0-50 m*	-	< 8 km
Cost 231	150-2000 MHz	4-50 m	1-3 m	0.2-50 km
SUI	< 11000 MHz	15-40 m	2-10 m	< 10 km
Okumura-Hata	150-1900 MHz	30-200 m	1-10 m	1-20 km
Ericsson	150-1900 MHz	20-200 m	1-5 m	0.2-100 km

* Above average rooftop level.

1) 3GPP Model

This propagation model is applicable for macro cells in urban and suburban areas outside the high-rise core, where the buildings are characterized by nearly uniform height. The resulting path loss is defined as:

$$L = 40(1 - 4 \cdot 10^{-3} h_b) \log_{10}(d) - \\ - 18 \log_{10}(h_b) + 21 \log_{10}(f) + 80, \quad (1)$$

where d represents the distance between the BS and ED, f is the carrier frequency in MHz, and h_b denotes the height of BS above average rooftop level. The 3GPP path loss model is valid for h_b ranging from 0 to 50 m with BS–ED separation from a few hundred meters to kilometers. For shorter distances, the model is not particularly accurate [14].

2) COST 231 Model

This propagation model originated as a combination of the Walfisch-Bertoni model and the final building path loss from the Ikegami Model [17]. The model is suitable for macrocells in urban and suburban environments operating with frequencies from 800 to 2000 MHz. The BS height can be in the interval from 4 to 50 m with ED height between 1 and 3 m. The distance between BS and ED may range from 0.2 up to 50 km [15].

For the line of sight (LOS) conditions, the mean path loss is defined as:

$$L_0 = 32.4 + 20 \log_{10}(d) + 20 \log_{10}(f), \quad (2)$$

where d represents the distance between BS and ED, and f denotes the carrier frequency. In the case of non-line of sight propagation (NLOS), the resulting path loss is expressed as a combination of free-space loss L_0, the roof-to-street loss L_{rts}, and multiscreen diffraction loss L_{msd}. The basic propagation loss is given by:

$$L = \begin{cases} L_0 + L_{rts} + L_{msd}, & L_{rts} + L_{msd} > 0 \\ L_0, & L_{rts} + L_{msd} \leq 0 \end{cases}, \quad (3)$$

where L_{rts} is computed according to the Ikegami model as:

$$L_{rts} = -8.2 - 10 \log_{10}(w) + 10 \log_{10}(f) + \\ + 20 \log(\Delta h_m) + L_{ori}, \quad (4)$$

while Δh_m represents the difference between average rooftop level h_r and mobile station antenna height h_m. The remaining parameter w denotes street width, and L_{ori} is a correction factor that accounts for loss due to street orientation angle φ:

$$L_{ori} = \begin{cases} -10 + 0.354\varphi, & 0^\circ \leq \varphi < 35^\circ \\ 2.5 + 0.075(\varphi - 35), & 35^\circ \leq \varphi < 55^\circ \\ 4.0 - 0.114(\varphi - 55), & 55^\circ \leq \varphi \leq 90^\circ \end{cases}. \quad (5)$$

The multiscreen diffraction loss L_{msd} is defined as:

$$L_{msd} = L_{bsh} + k_a + k_d \log_{10}(d) + \\ + k_f \log_{10}(f) - 9 \log_{10}(b), \quad (6)$$

where b represents mean separation between buildings, and the parameter L_{bsh} is dependent on the difference between BS height h_b and average rooftop level:

$$L_{bsh} = \begin{cases} -18 \log_{10}(1 + \Delta h_b) & \text{for} \quad h_b > h_r \\ 0 & \text{for} \quad h_b \leq h_r \end{cases}. \quad (7)$$

The coefficients k_a, k_d, and k_f are defined as follows:

$$k_a = \begin{cases} 54, & h_b > h_r \\ 54 - 0.8\Delta h_b, & h_b \leq h_r,\ d \geq 0.5\,\text{km} \\ 54 - 0.8\Delta h_b \frac{d}{0.5}, & h_b \leq h_r,\ d < 0.5\,\text{km} \end{cases}, \quad (8)$$

$$k_d = \begin{cases} 18, & h_b > h_r \\ 18 - 15\frac{\Delta h_b}{h_r}, & h_b \leq h_r \end{cases}, \quad (9)$$

$$k_f = \begin{cases} -4 + 0.7\left(\frac{f}{925} - 1\right), & \text{Medium cities} \\ -4 + 1.5\left(\frac{f}{925} - 1\right), & \text{Metropolitan centers} \end{cases}. \quad (10)$$

3) SUI Model

This propagation model originated as an extension to the Erceg model based on the measurement campaign conducted by AT&T Wireless group [18]. To calculate median path loss, SUI categorizes the environment into three groups based on the terrain morphology. Category A is intended to describe the hilly environment with high tree density resulting in high path loss. On the other hand, category C refers to the flat terrain with low tree density resulting in the minimum propagation losses. However, in our work, we use category B suited for the hilly environment with rare vegetation (intermediate path loss conditions).

The SUI model is suitable for cells smaller than 10 km in radius with BS antenna height in the range from 15 to 40 m. The height of the receiver antenna can vary from 2 to 10 m [12]. Finally, the path loss value is defined as:

$$L = \begin{cases} 20 \log_{10}\left(\frac{4\pi d}{\lambda}\right) & \text{for} \quad d \leq d_0' \\ A + 10\gamma \log_{10}\left(\frac{d}{d_0}\right) & \text{for} \quad d > d_0' \\ + {}_\Delta L_{bf} + {}_\Delta L_{bh} & \end{cases}, \quad (11)$$

where d represents the distance between BS and ED, d_0 is a reference distance of 100 m with corresponding path loss A, λ is the signal wavelength, and γ denotes path loss exponent. The frequency and receiver antenna correction factors are denoted as ${}_\Delta L_{bf}$ and ${}_\Delta L_{bh}$, respectively. The extended SUI model modifies the antenna correction factor resulting in modified reference distance d_0' calculated as:

$$d_0' = d_0 10^{-\left(\frac{{}_\Delta L_{bf} + {}_\Delta L_{bh}}{10\gamma}\right)}. \quad (12)$$

The remaining parameters of the propagation model are

computed as follows:

$$A = 20\log_{10}\left(\frac{4\pi d_0'}{\lambda}\right), \quad \gamma = a - bh_b + \frac{c}{h_b}, \tag{13}$$

where h_b denotes BS height, and a, b, c represent constants dependent on the terrain category, see Table 3.

TABLE 3: SUI model parameters.

	Category A	Category B	Category C
a	4.6	4.0	3.6
b	0.0075	0.0065	0.005
c	12.6	17.1	20

The remaining correction factors for receiver antenna height $h \leq 3$ m are defined as:

$$\Delta L_{bf} = 6\log_{10}\left(\frac{f}{2000}\right), \; \Delta L_{bh} = -10\log_{10}\left(\frac{h}{3}\right). \tag{14}$$

4) Okumura-Hata Model

The propagation model based on the extensive measurements carried out in Tokyo, giving the median value of the propagation loss. It can be used for frequencies from 150 up to 1500 MHz with inter-transceivers distance ranging between 1 and 20 km. The model is valid for BS height from 30 to 200 m with ED elevation from 1 to 10 m. The basic propagation loss is expressed as [10], [19]:

$$\begin{aligned} L_b = {} & 69.55 + 26.16\log_{10}(f) - 13.82\log_{10}(h_b) - \\ & - a(h_m) + (44.9 - 6.55\log_{10}(h_b))\log_{10}(d_m), \end{aligned} \tag{15}$$

where f is the carrier frequency, h_b denotes BS height, h_r stands for ED antenna height, and d represents the distance between transceivers. The remaining parameter $a(h_m)$ represents the correction factor for ED antenna. For large cities with $f > 200$ MHz is computed as follows:

$$a(h_m) = 3.2\log_{10}(11.75h_m)^2 - 4.79. \tag{16}$$

Based on the above-mentioned expressions, the rural areas path loss formula is defined as:

$$L = L_b - 4.78\log_{10}(f)^2 + 18.33\log_{10}(f) - 40.94. \tag{17}$$

5) Ericsson Model

It is an improvement of the Okumura-Hata propagation model with adjustment for different morphology types. The model is verified for the frequency range from 150 MHz to 2 GHz with BS height ranging from 20 to 200 m. The antenna of the receiver may vary from 1 to 5 m. This model is targeted for macro sites with a cell radius between 0.2 and 100 km [16]. The resulting path loss is estimated according to the formula below:

$$\begin{aligned} L = {} & a_0 + a_1\log_{10}(d) + a_2\log_{10}(h_b) + a_3\log_{10}(h_b) \times \\ & \times \log_{10}(d) - 3.2\log_{10}(11.75h_r)^2 + g(f), \end{aligned} \tag{18}$$

where h_b represents BS antenna height, h_r is the ED antenna height, f denotes the carrier frequency, and d stands for inter BS–ED distance. The parameters a_0–a_3 are constants dependent on the selected propagation environment, see Table 4. Finally, the frequency correction factor $g(f)$ is defined as:

$$g(f) = 44.49\log_{10}(f) - 4.78\log_{10}(f)^2. \tag{19}$$

TABLE 4: Ericsson model constants.

Environment	a0	a1	a2	a3
Urban	36.2	30.2	-12	0.1
Suburban	43.2	68.93	-12	0.1
Rural	45.95	100.6	-12	0.1

C. BEYOND STATE-OF-THE-ART

Considering all the propagation models with the same input parameters plotted side-by-side in Fig. 1, one may observe that the diversity between their results is significant. The maximum difference between the models at low distance values is almost 35 dB, but then gradually decreases reaching 22 dB at 4 km distance.

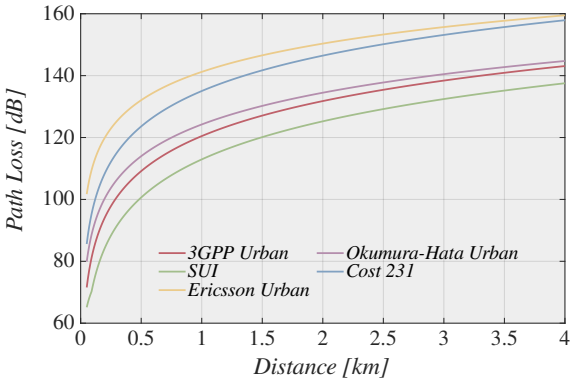

FIGURE 1: Comparison of propagation models.

Out of all the considered models, the SUI model provides the most optimistic predictions. The main reason is the selected terrain category, as the type B morphology is intended for suburban environments. The SUI curve also reveals that up to distance d_0 (0.09 km), the propagation follows the free space model characteristics. This behavior is in line with the results given by the formula (11). The performance of 3GPP and Okumura-Hata Urban models is comparable for the inter BS-ED distances in the order of few kilometers. On the greater distances, the 3GPP model has tendencies to predict higher path loss values. In the case of the COST 231, it is clear that the model considers additional losses due to the building data. This model is suitable when the dominant energy is contributed over the rooftops diffraction, however, the benefits of this effect vanish with the increasing distance [20]. As a result, the model produces the steepest path loss curve. Finally, the Ericsson Urban model provides the most pessimistic path loss prediction. Nevertheless, these pessimistic predictions are caused by the high path loss at the initial point. Contrary, the slope of the curve is the lowest.

It is necessary to bear in mind that all these models are empirical, i.e., based on the measurement campaigns. Due to this fact, the propagation models may indicate inaccurate

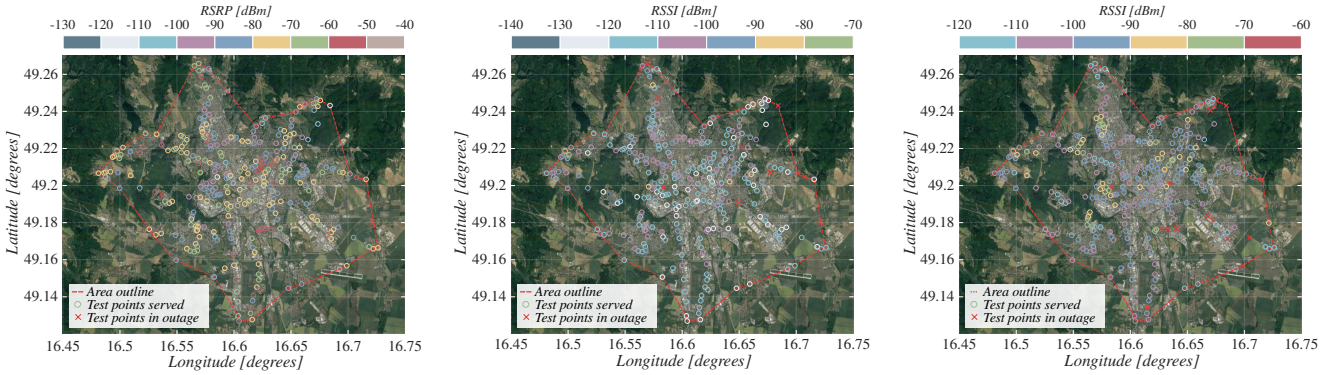

(a) NB-IoT **(b) Sigfox** **(c) LoRaWAN**

FIGURE 2: Coverage by LPWAN technologies in the city of Brno.

results in areas with different geographical position or terrain morphology. For these reasons, it is necessary to fine-tune the propagation models to achieve the highest accuracy in specific environmental conditions. In the following section, the considered propagation models are tuned to fit the measurement data obtained in the city of Brno in the Czech Republic. To verify the accuracy of the tuned models, we cross-validate the data with measurement results acquired in the city of Ostrava.

IV. MEASUREMENT CAMPAIGN

To acquire a sufficient result set, we conducted a measurement campaign with over 300 unique test points in the city of Brno, see Fig. 2. Sigfox and LoRaWAN report the signal levels only in the form of received signal strength indicator (RSSI). Therefore, we utilize this parameter as the coverage quality indicator. NB-IoT, on the other hand, provides a variety of signal strength and quality parameters. In this research, we use reference signal received power (RSRP) as it provides more accurate signal power estimations by excluding interference from other sectors.

Further, we performed similar measurements covering 34 unique places in the city of Ostrava to obtain the validation data set. The test points were spread throughout the cities and co-allocated with the stop points of the public transport.

A. MEASUREMENT EQUIPMENT AND SETUP

For Sigfox and LoRaWAN coverage measurements, we utilized two commercial field network testers from the company Adenuis [21] operating in 868 MHz ISM, both equipped with 0 dBi omnidirectional antenna. Sigfox measurements were conducted utilizing Adenuis tester designated as ARF8121AA with the maximum radiated power set to 14 dBm to achieve the longest possible communication range. In the case of LoRaWAN, we utilized field network tester ARF8123AA from the same company. LoRaWAN tester employed maximal radiated power of 14 dBm with the SF12, and coding rate (CR) 4/5. This CR value does not provide the highest communication range, but it was selected due to the requirement imposed by the LoRaWAN specification documents for the EU region [11]. Even with such a low CR, the packet delivery ratio should not be noticeably affected as the study [22] suggests. On the other hand, the utilization of high CR like 4/8 heavily influences the number of collisions. According to the study [23], the difference is more than 20 %.

In case of NB-IoT, we used the testing device developed at the Brno University of Technology (BUT). It was equipped with the SARA N210 NB-IoT module from company uBlox operating in the 800 MHz (B20) frequency band [24]. The radio signal with a maximum power of 23 dBm was conveyed via a 2 dBi omnidirectional half-wave antenna.

All measurements in both cities followed the same pattern. The test devices were transferred to the selected location and positioned approximately one meter above ground level apart from any visible obstacles. When the testers were powered, each of them transferred 10 messages with a period of 30 s. The message size for each technology was set to 12 B reflecting the limitation of Sigfox technology. Once all the measurements were finished, we downloaded the available data for further analysis.

For all LPWA technologies in both cities, we utilized commercial networks consisting of multiple BSs. The exact location of the BSs are known to the authors but can not be published due to the non-disclosure agreement with network operators.

B. CITY-SCALE COVERAGE

As discussed above, our measurement campaign included two mid-size cities situated in the Czech Republic. From the perspective of both geographical topology and urban development, these two cities share similar properties. Thus we can expect comparable signal propagation, which allows us to independently cross-validate our results.

Measurements in the cities of Brno and Ostrava covered the area of 150 km^2, and 140 km^2, respectively. Even though the area size is similar, the measurement campaign conducted in Brno was more extensive, with 303 test points (only 34 in Ostrava). This imbalance in test points density is also reflected in average communication distance and the number

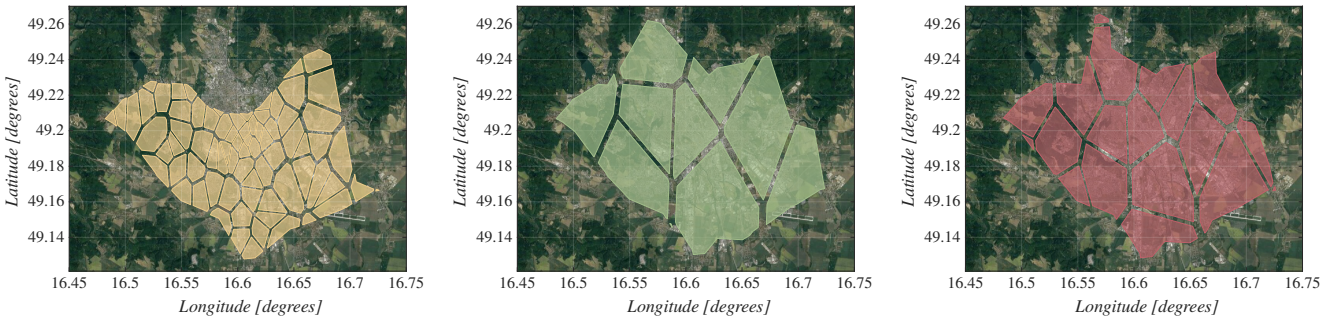

(a) NB-IoT **(b)** Sigfox **(c)** LoRaWAN

FIGURE 3: Voronoi diagram of LPWAN BSs in the city of Brno.

TABLE 5: Parameters of the city coverage.

LPWA Technology	Avg. BS-ED distance [km][1]		Number of BS [-]		Avg. signal level [dBm]	
	Brno	*Ostrava*	*Brno*	*Ostrava*	*Brno*	*Ostrava*
NB-IoT	0.52	0.53	78	31	-76	-79
Sigfox	3.45	5.27	13	16	-112	-118
LoRaWAN	1.86	3.97	19	16	-98	-105

[1] It is considered the distance to the closest BS.

of utilized BSs. As one can see from the Table 5, Ostrava's NB-IoT results include almost half as many BSs as Brno – with only 10 % of measurement points. It is mainly caused by a low density of measurement points in Ostrava, where the ED is connected to the different BS at each location. This fact is also supported by the higher deployment density of NB-IoT BSs in comparison with its competitors, Sigfox and LoRaWAN. For the latter mentioned technologies, the number of measurement points has a negligible effect on the number of utilized BS. From the perspective of signal levels, both cities show similar results. The higher propagation losses for Sigfox and LoRaWAN in Ostrava are caused by the longer average distance between BS and ED.

V. EVALUATION OF PROPAGATION MODELS

In this section, we first introduce the proposed methodology, associated algorithms, and model's quality assessment metrics. We then proceed by reporting the results, including model fitting and further cross-validation.

A. METHODOLOGY

Having sets of measurement data from two cities at our disposal, we propose the following methodology to fine-tune the propagation models. In the first step, we derive the fitted reference model from the data acquired during the measurement campaign. To this aim, we use the data received by all LoRaWAN and Sigfox BSs (multiple BSs can receive the message), but for NB-IoT, we can use only the data from the serving BS; therefore, the input data set is smaller. Then, we assess the accuracy of the propagation models defined in Section III comparing them with the fitted models to determine the ones having the closet approximation for Brno data. The selected models are further fine-tuned by changing the value of floating intercept (FI) to provide the best possible fit for the data [25]. Finally, we assess the accuracy of the tuned models by cross-validating the proposed models using the Ostrava data.

For each LPWAN technology, the fitted propagation model is derived from the measurement results utilizing the non-linear regression. The obtained path loss exponent further serves as an input of the log-distance path loss model denoted by:

$$L = \overline{L}(d_0) + 10\gamma \log_{10}\left(\frac{d}{d_0}\right), \tag{20}$$

where $\overline{L}(d_0)$ is the path loss at reference distance $d_0 = 0.1$ km (also represents the FI), γ is the path loss exponent, and d denotes the distance between BS and ED. The value of $\overline{L}(d_0)$ is calculated from the free-space path loss formula with an additional 10 dB attenuation reflecting the propagation losses in the urban environment [19].

When the fitted propagation models are derived, we can continue the fine-tuning of the verified models. This process consists of two main phases. First, the models are fine-tuned based on a visual estimation. In other words, the validated model FI is shifted to be as close to the fitted model as possible (such a model is then called fine-tuned). When this process is finished, the cumulative deviation formula (21) is used to evaluate fine-tuned model accuracy. For the maximum accuracy, the fine-tuned model FI is moved by the difference Δ, and the quality factor is recomputed again. If the value of the quality factor is smaller than the previous one, the whole process is repeated until the lowest possible mean deviation is found.

To facilitate a quantitative comparison between the model and measurement data, we propose to use the averaged metric specifying the cumulative relative deviation, i.e.,

$$Q = \frac{1}{N}\sum_{i=1}^{N}\frac{\left|R_i^{(1)} - R_i^{(2)}\right|}{\left|R_i^{(2)}\right|}, \tag{21}$$

where $R_i^{(1)}$ and $R_i^{(2)}$ are the sample values of fitted and verified models at exactly the same point, N is the overall number of considered measurement points. Note that the modulus is used to account for positive and negative deviations.

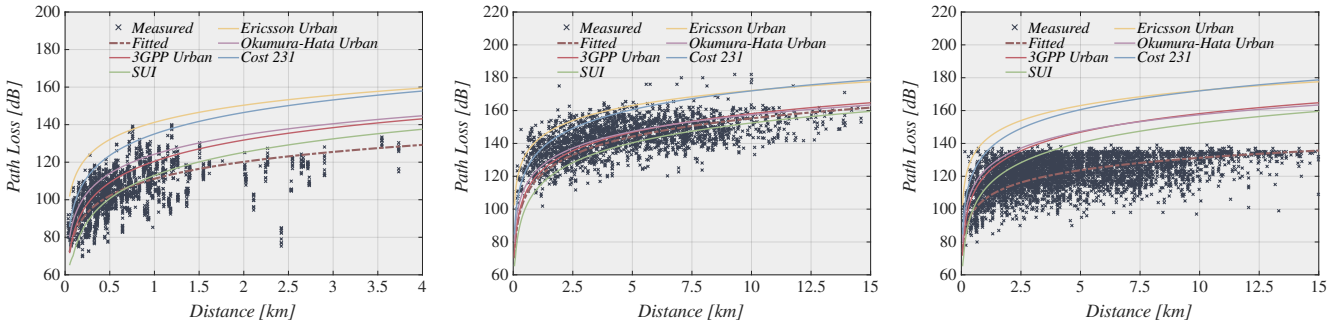

(a) NB-IoT **(b) Sigfox** **(c) LoRaWAN**

FIGURE 4: Comparison of measured data with standardized path loss models for city of Brno.

As one may observe, the averaged integral metric specified in (21) is independent of the number of points N, where the coverage metric is evaluated and produces the absolute deviation from the actual coverage averaged over all the considered measurement points.

The process of quantitative comparison is not a single operation but consists of several subroutines. First, the BS locations serve as the input of the Voronoi diagram. It provides partitioning of the plane into regions containing one generating point, and each point in a given region is closer to this generating point than to any other [26]. The resulting tessellated areas for each technology are depicted in Fig. 3. The figure illustrates the tremendous differences in BS deployment density, especially, for NB-IoT and Sigfox.

The tessellated area is then divided into a regular 50 m grid with each cell serving as one measurement point of the formula (21). The distance of such measurement point to the closest BS is used as an input parameter of the fitted and fine-tuned propagation models.

B. MODEL FITTING

We now proceed with the first two steps in the proposed methodology, i.e., selection of the best models for each of the considered technology and further tuning of the selected model to Brno data.

First, we asses the quality of approximation provided by propagation models defined in Section II. To this aim, Fig. 4 shows the Brno measurement data complemented by the fitted models and all the verified propagation models in the basic form. Cursory visual analysis suggests that 3GPP Urban, Okamura-Hata Urban, and SUI models can be considered as promising candidates for accurate approximation while the rest of the models overestimate the measured data. Further, to verify our visual observations, we apply the quantitative formula in the form of (21) and obtain the mean deviation between the fitted (based on measured data) and referenced models. As depicted in Fig. 5, the numerical results match the prediction based on visual observations. The SUI model provides the most accurate results for both NB-IoT and LoRaWAN, while the 3GPP model characterizes Sigfox the best. Nevertheless, these values are gathered from the verified propagation models in their basic form.

In the next step, our analysis continues by fine-tuning the selected verified propagation models to transcribe the generic log-distance path loss model in the form (20) based on the Brno data. The results of this operation, i.e., side by side comparison of the fitted models with fine-tuned counterparts, are depicted in Fig. 6. Analyzing the data presented in the figure one may observe, that for NB-IoT and LoRaWAN technologies, even the fine-tuned models slightly deviate from the fitted ones. The major difference is observed for large BS-ED separation distances, i.e., larger than 1 km for NB-IoT, and larger than 2.5 km for LoRaWAN. The only exception, in the case of NB-IoT technology, is the Ericsson Urban model that shows quite an accurate match for all the considered distances. For Sigfox technology, the best match with the fitted model is visible at the 3GPP Urban and SUI models. In the case of LoRaWAN, the Ericsson Urban model provides the highest accuracy even though there is a visible divergence from the fitted model for larger distances.

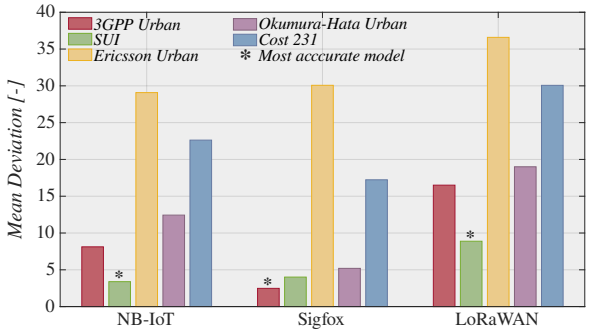

FIGURE 5: Propagation models accuracy in the city of Brno.

To quantitatively assess the accuracy of the fine-tuned models, we demonstrate the averaged deviations of the fine-tuned models from the fitted data in Fig. 7. As one may observe, the fine-tuned Ericsson Urban model indeed drastically outperforms other models for LoRaWAN and, especially, for NB-IoT technology. Similar conclusions can be stated about the 3GPP Urban model in the case of Sigfox technology. The best performing models for each LPWAN technology are also highlighted in the Table 6. Surprisingly, if we compare the results depicted in Figs. 5 and 6, the Ericsson Urban model

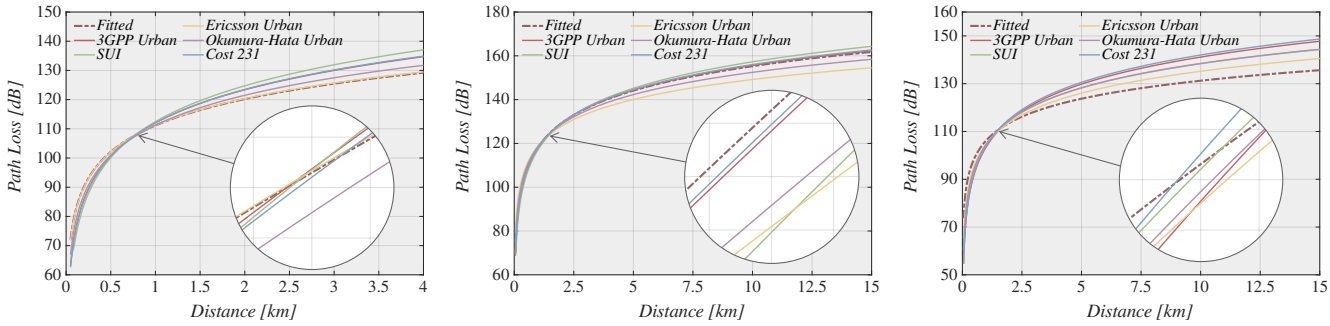

(a) NB-IoT **(b) Sigfox** **(c) LoRaWAN**

FIGURE 6: Comparison of fitted model with fine-tuned path loss models for city of Brno.

moves from the least to the most accurate model for both NB-IoT and LoRaWAN. In the case of NB-IoT, the accuracy of the Ericsson model is improved almost 400 times. For LoRaWAN, it is still an impressive 36 fold accuracy increase. On the other hand, there is no change for Sigfox, with the 3GPP model still providing the best approximation.

Moreover, if we compare the best performing verified models in the basic form with any fine-tuned one, the tuned models still clearly dominate. The best fine-tuned model for NB-IoT displays the 100 times accuracy increase followed by the 20 fold increase in the case of Sigfox. Finally, LoRaWAN holds the last place with 8 times accuracy increase.

TABLE 6: Parameters of tuned propagation models.

Propagation Model	NB-IoT		Sigfox		LoraWAN	
	PL_{d0}	γ	PL_{d0}	γ	PL_{d0}	γ
3GPP	112.07	3.76	118.04	3.76	103.54	3.76
SUI	112.43	4.09	117.09	4.02	102.35	3.89
Ericsson Urban	111.21	3.04	118.82	3.04	104.82	3.04
Hata Urban	111.22	3.41	118.33	3.38	104.69	3.33
COST 231	112.03	3.80	118.00	3.80	104.00	3.80

As the results presented in Fig. 6 provide only a graphical representation of the fine-tuned models, for the sake of traceability and repeatability of our results, we list the underlying parameters or the fine-tuned models in Table 6. The parameters are presented in the form log-distance path loss model, i.e., FI PL_{d0} and path loss exponent γ. The colour-highlighted cells represent the most accurate models.

C. MODELS CROSS-VALIDATION

The most critical question in propagation modeling is related to the applicability of the developed models to other deployments. We now proceed to perform cross-validation of the identified best fine-tuned models based on the Brno measurements using the Ostrava data.

To perform the cross-validation, we first use the models fine-tuned on Brno data and plot them against the Ostrava data together with the model fitted on Ostrava data, see Fig. 8. Analyzing the presented data, it is clear that all the Brno tuned models potentially provide an accurate approximation for NB-IoT technology, but the Ericsson Urban model significantly outperforms the rest of the competitors. In the case of LoRaWAN and Sigfox technologies, the Brno fine-tuned models generally capture the behavior of the path loss for shorter distances much better compared to the larger separation distances between ED and BS. Nevertheless, the Okamura-Hata Urban models seem to provide a close match for the Sigfox. Unfortunately, for LoRaWAN, the deviation of the Brno fine-tuned model is significantly larger. Here, the Ericsson Urban model catches the path-loss characteristics the best.

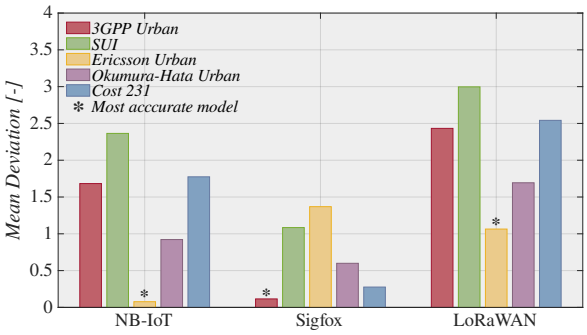

FIGURE 7: Tuned models accuracy in the city of Brno.

In order to numerically quantify the performance of the models, Fig. 9 provides the comparison of all Brno fine-tuned models with the Ostrava fitted ones. For each LPWAN technology, the best performing reference (not-tuned) propagation model is also displayed. The assessment is based on averaged coverage metric defined in (21). The most accurate reference (not-tuned) model for each technology in Ostrava is the SUI model. Such a finding is in line with reference models in Brno, where the SUI model provides the best accuracy for NB-IoT and LoRaWAN, and for Sigfox it holds the second place.

Further analysis of the results indicates that, in general, the approximation for LoRaWAN technology is less precise compared to NB-IoT and Sigfox. In the case of NB-IoT, even the best performing reference (not-tuned) model does not give as accurate results as the worst model fine-tuned with Brno data. In line with that, the best performing Brno fine-tuned model provides a 30-fold accuracy improvement over the most accurate reference (not-tuned) model. Surprisingly,

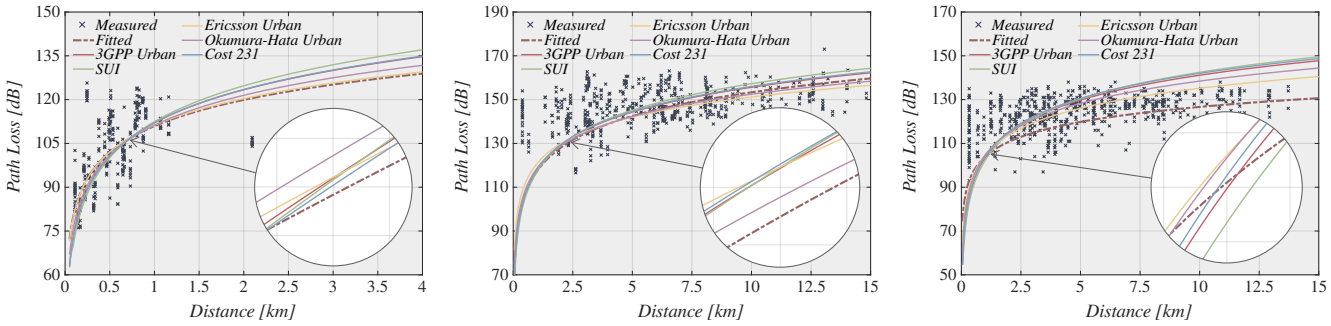

(a) NB-IoT **(b) Sigfox** **(c) LoRaWAN**

FIGURE 8: Comparison of fitted model derived from Ostrava data and models tuned to Brno data.

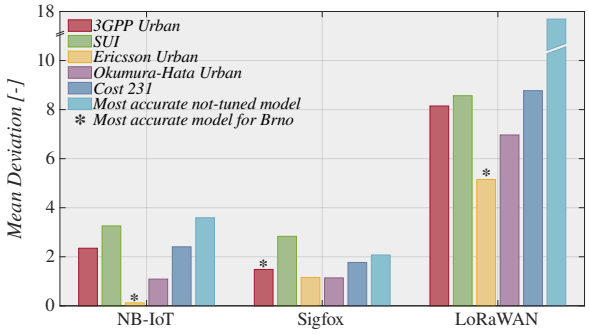

FIGURE 9: Models cross-validation in the city of Ostrava.

for Sigfox, the best performing model in Ostrava (Okumura-Hata Urban) differs from Brno (3GPP). The difference is only marginal, with a value slightly above 0.3 dB ($\approx$ 23%). Still, all the Brno fine-tuned models, except the SUI, outperform even the best reference (not-tuned) model. Despite the decreased accuracy of Brno fine-tuned models on Ostrava data for LoRaWAN technology, all of them still provide higher precision than the reference (not-tuned) ones. Numerically, the best Brno-tuned model offers 9 times lower approximation error compared to the best performing reference (not-tuned) model.

VI. CONCLUSIONS

Aiming at developing an accurate model for urban environments for all major LPWAN technologies, including Sigfox, LoRaWAN, and NB-IoT, we have proposed two-step methodology based on fitting and cross-validation. In the first step, we have considered five major LPWAN propagation models (3GPP, SUI, Ericsson Urban, Okumura-Hata Urban, and COST 231) available to date and identified the best candidates based on the fine tuning of models parameters for a set of data. In the second stage, we validated the selected models using another measurement data set.

Our numerical results demonstrate that none of the reference models proposed so far can be used "as is" and have to be fine-tuned to match the propagation specifics of the urban environment. The tuned Ericcson Urban models are observed to provide the best approximation for NB-IoT and LoRaWAN technologies, while the 3GPP Urban model is the best choice for Sigfox. The cross-validation using a separate set of data from another urban environment has shown that the proposed tuned models provide at least as accurate approximation as those models specifically tuned for the environment of interest. In the case of NB-IoT, the best-performing fine-tuned model provides 30 times better performance than the most accurate reference model in the basic form. The smallest difference is visible for Sigfox, where the tuned model provides a 40 % accuracy increase. The highest growth of inaccuracy is visible for LoRaWAN technology, where the average deviation of Brno fine-tuned models increased almost 8 times. Regardless, the tuned models provide nearly three times higher accuracy compared to the best reference model in the basic form. This allows us to conclude that these tuned models can be safely used for the planning of LPWAN deployments in urban conditions.

REFERENCES

[1] O. Liberg, Cellular Internet of Things, 1st ed. Cambridge: Elsevier, 2019.
[2] A. Hoglund, X. Lin, O. Liberg, A. Behravan, E. A. Yavuz, M. Van Der Zee, Y. Sui, T. Tirronen, A. Ratilainen, and D. Eriksson, "Overview of 3GPP Release 14 Enhanced NB-IoT," IEEE Network, vol. 31, no. 6, pp. 16–22, November 2017.
[3] Sigfox, "Sigfox Connected Objects: Radio Specifications," Sigfox, Ref.: EP-SPECS, Rev.: 1.4, November 2019.
[4] A. Lavric, A. I. Petrariu, and V. Popa, "Long Range SigFox Communication Protocol Scalability Analysis Under Large-Scale, High-Density Conditions," IEEE Access, vol. 7, pp. 35 816–35 825, 2019.
[5] LoRa Alliance™, "LoRaWAN™ 1.0.3 Specification," LoRa Alliance™, Final release, July 2018.
[6] D. Magrin, M. Capuzzo, and A. Zanella, "A Thorough Study of LoRaWAN Performance Under Different Parameter Settings," IEEE Internet of Things Journal, vol. 7, no. 1, pp. 116–127, 2020.
[7] K. Mekki and E. Bajic and F. Chaxel and F. Meyer, "A Comparative Study of LPWAN Technologies for Large-Scale IoT Deployment," ICT Express, vol. 5, no. 1, pp. 1–7, 2019, Available from: http://www.sciencedirect.com/science/article/pii/S2405959517302953.
[8] R. El Chall, S. Lahoud, and M. El Helou, "LoRaWAN Network: Radio Propagation Models and Performance Evaluation in Various Environments in Lebanon," IEEE Internet of Things Journal, vol. 6, no. 2, pp. 2366–2378, 2019.
[9] E. Teng, J. Falcao, C. Ruiz, F. Mokaya, P. Zhang, and B. Iannucci, "Aerial Sensing and Characterization of Three-Dimensional RF Fields," in Second International Workshop on Robotic Sensor Networks, 04 2015.
[10] E. Harinda, S. Hosseinzadeh, H. Larijani, and R. M. Gibson, "Comparative Performance Analysis of Empirical Propagation Models for LoRaWAN 868 MHz in an Urban Scenario," in 2019 IEEE 5th World Forum on Internet of Things (WF-IoT), April 2019, pp. 154–159.
[11] LoRa Alliance®, "RP002-1.0.1® Regional Parameters," LoRa Alliance®, Final, February 2020.

[12] V. S. Abhayawardhana, I. J. Wassell, D. Crosby, M. P. Sellars, and M. G. Brown, "Comparison of Empirical Propagation Path Loss Models for Fixed Wireless Access Systems," in 2005 IEEE 61st Vehicular Technology Conference, vol. 1, May 2005, pp. 73–77 Vol. 1.

[13] T. S. Rappaport, A. Annamalai, R. Buehrer, and W. H. Tranter, "Wireless communications: past events and a future perspective," IEEE communications Magazine, vol. 40, no. 5, pp. 148–161, 2002.

[14] 3GPP, "LTE; Evolved Universal Terrestrial Radio Access (E-UTRA); User Equipment (UE) radio transmission and reception (3GPP TS 36.101 version 15.3.0 Release 15)," 3GPP, ETSI TS 136 101, October 2018.

[15] E. Damosso, Digital Mobile Radio Towards Future Generation Systems, 1st ed. Brussels,: Directorate-General Telecommunications, Information society, Information Market, and Exploitation of Research, 1999.

[16] A. El-Nashar, M. El-Saidny, and M. Sherif, Design, Deployment and Performance of 4G-LTE Networks: A Practical Approach, 1st ed. Wiley Publishing, 2014.

[17] L. M. Correia, "A View of the COST 231-Bertoni-Ikegami Model," in 2009 3rd European Conference on Antennas and Propagation, March 2009, pp. 1681–1685.

[18] V. Erceg, L. J. Greenstein, S. Y. Tjandra, S. R. Parkoff, A. Gupta, B. Kulic, A. A. Julius, and R. Bianchi, "An Empirically Based Path Loss Model for Wireless Channels in Suburban Environments," IEEE Journal on Selected Areas in Communications, vol. 17, no. 7, pp. 1205–1211, July 1999.

[19] A. Ikpehai, B. Adebisi, K. M. Rabie, K. Anoh, R. E. Ande, M. Hammoudeh, H. Gacanin, and U. M. Mbanaso, "Low-Power Wide Area Network Technologies for Internet-of-Things: A Comparative Review," IEEE Internet of Things Journal, vol. 6, no. 2, pp. 2225–2240, April 2019.

[20] D. Har, A. M. Watson, and A. G. Chadney, "Comment on Diffraction Loss of Rooftop-to-street in COST 231-Walfisch-Ikegami Model," IEEE Transactions on Vehicular Technology, vol. 48, no. 5, pp. 1451–1452, 1999.

[21] Adeunis, "FTD: Network Tester," Available from: https://www.adeunis.com, accessed: 2020-05-14.

[22] A. M. Yousuf, E. M. Rochester, B. Ousat, and M. Ghaderi, "Throughput, Coverage and Scalability of LoRa LPWAN for Internet of Things," in 2018 IEEE/ACM 26th International Symposium on Quality of Service (IWQoS), 2018, pp. 1–10.

[23] A. Lavric and V. Popa, "Performance Evaluation of LoRaWAN Communication Scalability in Large-Scale Wireless Sensor Networks," Wireless Communications and Mobile Computing, vol. 2018, p. 6730719, Jun 2018. [Online]. Available: https://doi.org/10.1155/2018/6730719

[24] u Blox, "SARA-N2 Modules AT Commands Manual," Available from: https://www.u-blox.com, accessed: 2020-05-14.

[25] M. Bahjat, T. Rahman, O. Abdul Aziz, M. Hindia, and E. Hanafi, "Channel Characterization and Path Loss Modeling in Indoor Environment at 4.5, 28, and 38 GHz for 5G Cellular Networks," International Journal of Antennas and Propagation, vol. 2018, pp. 1–14, 09 2018.

[26] X. Wang, Z. Tian, W. Wang, F. He, L. Zhao, and P. Gao, "A Novel Algorithm for Barrier Coverage Based on Hybrid Wireless Sensor Nodes," IEEE Access, vol. 7, pp. 118 866–118 875, 2019.